Identifying imaging genetic associations via regional morphometricity estimation

Jingxuan Bao[1][*], Zixuan Wen[1][*], Mansu Kim[1], Andrew J. Saykin[2], Paul M. Thompson[3], Yize Zhao[4], Li Shen[1][†], and for the Alzheimer's Disease Neuroimaging Initiative[‖]

[1]*Department of Biostatistics, Epidemiology and Informatics*
University of Pennsylvania Perelman School of Medicine, Philadelphia, PA 19104, USA
[2]*Indiana Alzheimer Disease Center, Department of Radiology and Imaging Sciences*
Indiana University School of Medicine, Indianapolis, IN 46202, USA
[3]*Imaging Genetics Center, Stevens Institute for Neuroimaging and Informatics*
University of Southern California School of Medicine, Marina del Rey, CA 90292, USA
[4]*Department of Biostatistics*
Yale University School of Public Health, New Haven, CT 06511, USA
[†]*E-mail: li.shen@pennmedicine.upenn.edu*

Brain imaging genetics is an emerging research field aiming to reveal the genetic basis of brain traits captured by imaging data. Inspired by heritability analysis, the concept of morphometricity was recently introduced to assess trait association with whole brain morphology. In this study, we extend the concept of morphometricity from its original definition at the whole brain level to a more focal level based on a region of interest (ROI). We propose a novel framework to identify the SNP-ROI association via regional morphometricity estimation of each studied single nucleotide polymorphism (SNP). We perform an empirical study on the structural MRI and genotyping data from a landmark Alzheimer's disease (AD) biobank; and yield promising results. Our findings indicate that the AD-related SNPs have higher overall regional morphometricity estimates than the SNPs not yet related to AD. This observation suggests that the variance of AD SNPs can be explained more by regional morphometric features than non-AD SNPs, supporting the value of imaging traits as targets in studying AD genetics. Also, we identified 11 ROIs, where the AD/non-AD SNPs and significant/insignificant morphometricity estimation of the corresponding SNPs in these ROIs show strong dependency. Supplementary motor area (SMA) and dorsolateral prefrontal cortex (DPC) are enriched by these ROIs. Our results also demonstrate that using all the detailed voxel-level measures within the ROI to incorporate morphometric information outperforms using only a single average ROI measure, and thus provides improved power to detect imaging genetic associations.

Keywords: Brain imaging genetics; Regional morphometricity; Alzheimer's Disease

---

1. Introduction

Brain imaging genetics studies genetics using imaging as phenotype in order to reveal the underlying genetic basis of neurobiological traits and phenotypes.[1] It aims to examine how the difference in genetic markers such as single nucleotide polymorphisms (SNPs) affect brain structure, function or connectivity[2] quantified by features extracted from multimodal brain imaging data. Thanks to the recent advances in multimodal neuroimaging and high throughput genotyping technologies, there appears a large body of literature in this field to investigate genetic and molecular pathways behind brain imaging phenotypes.[3–7]

Heritability[8] is an important measurement in brain imaging genetic studies. It quantifies the proportion of the total variance of imaging quantitative traits (QTs) explained by genetic variants, which is able to help rank and prioritize heritable imaging QTs and provide guidance for subsequent imaging genetic association studies. A recent study adapted the concept of heritability and proposed a new global measurement of anatomical signature for a given trait to quantify the proportion of trait variation which can be explained by whole-brain morphology, and this measure is named as "morphometricity". It offers a novel strategy to assess the neuroanatomical correlation of the trait and their underlying associations.[9] Morphometricity analysis has been applied and helped researchers detect the associations that cannot be captured by traditional statistical models.[10–13]

In this study, we extend the concept of morphometricity from its original definition at the whole brain level to a more focal level based on a region of interest (ROI). We propose a novel strategy to identify the SNP-ROI association via regional morphometricity estimation of each SNP, which can serve as an alternative strategy to the traditional association models used in the genome-wide association studies (GWAS). To capture the ROI-level morphometric information and discover the ROI-level brain imaging genetic associations, a typical choice is to define imaging QTs using ROI-level summary statistics. However, the detailed voxel-level signals are ignored with the use of the ROI-level QTs. To bridge this gap, in this work, we propose a voxel based method, which is able to capture more detailed information when performing the imaging genetic association studies via regional morphometricity estimation, and thus provides improved power for association detection.

The rest of the paper is organized as follows. We introduce morphometricity estimation in Section 2, discuss our data and materials in Section 3, describe our experimental design in Section 4, present and discuss our results in Section 5, and conclude the paper in Section 6.

2. Methods

Given a trait, its morphometricity is defined as the proportion of the trait variation that can be explained by brain morphology (e.g., as captured by measurements derived from structural brain MRI scans). The primary aim of morphometricity analysis is to examine and globally quantify the statistical association between a trait and all the studied morphometric measures (e.g., the whole brain anatomical signature of a trait[9]), rather than identifying one or more specific morphometric measures associated with the trait.

Morphometricity[9] is grounded in linear mixed effects (LME) modeling:

$$y = X\beta + a + \varepsilon, \tag{1}$$

where y is an $N \times 1$ vector of a trait with N being the number of subjects, β is the vector of fixed effects, X is the matrix of confounding variables, a is an $N \times 1$ vector of trait variants with $a \sim N(0, K_a \sigma_a^2)$, and $\varepsilon \sim N(0, I\sigma_\varepsilon^2)$ is the error term. I is the identity matrix. K_a is interpreted as a scaled anatomic similarity matrix (ASM). Entries in the ASM quantify the pairwise global similarity between the brain morphologies of two individuals. There are two widely used kernels (linear and Gaussian) to construct the ASM. In this study, we use a Gaussian kernel on standardized imaging features, with the (i, j)-th entry defined as

$$\exp\left(-\sum_k \frac{(v_{ik} - v_{jk})^2}{Ms_k^2}\right),$$

where v_{ik} denotes the k-th imaging measurement from subject i, M is the total number of measurements, and s_k is the sample SD of the k-th measurement.

Morphometricity[9] is defined as

$$m^2 = \frac{\sigma_a^2}{\sigma_a^2 + \sigma_\varepsilon^2} = \frac{\sigma_a^2}{\sigma_y^2}, \tag{2}$$

where σ_y^2 is the total trait variance. The LME model has already been implemented in the morphometricity tool available at `people.csail.mit.edu/msabuncu/morphometricity/`. In this work, we slightly modify this tool by adding an implementation of the significance or p-value estimation using a likelihood ratio test,[9] and apply it to compute two variants of the regional morphometricity for all the studied genetic traits.

Instead of computing global morphometricity at the whole brain level, we calculate regional morphometricity at the ROI level. Given an ROI and a SNP (i.e., a genetic trait), we propose to calculate the ROI-based regional morphometricity of the SNP to examine the SNP-ROI association. To achieve this goal, we design two approaches to calculate the ASM:

- Approach 1: We extract a single ROI measure for each subject (i.e., average of all the voxel measures in the ROI; see Figure 1(d)), and use that to compute the ASM.
- Approach 2: We calculate the ASM using all the voxel measures with the ROI (see Figure 1(e)).

We anticipate that the second strategy will capture the ASM more accurately than the first strategy, and thus have improved power to detect imaging genetic associations.

3. Materials

The genotypinig data, demographic data and imaging data used in the preparation of this article were obtained from the Alzheimer's Disease Neuroimaging Initiative (ADNI) database (adni.loni.usc.edu).[14–16] The ADNI was launched in 2003 as a public-private partnership, led by Principal Investigator Michael W. Weiner, MD. The primary goal of ADNI has been to test whether serial magnetic resonance imaging (MRI), positron emission tomography (PET), other biological markers, and clinical and neuropsychological assessment can be combined to measure the progression of mild cognitive impairment (MCI) and early Alzheimer's disease (AD). Up-to-date information about the ADNI is available at `www.adni-info.org`.

Table 1: **Participant characteristics.** Total number of subjects, age, and sex are shown in this table. The mean ± sd for the age of all subjects within each diagnosis group are reported. The number of male/female subjects within each diagnosis group is also reported.

Diagnosis	CN	SMC	EMCI	LMCI	AD	Overall
Number	341	85	265	495	286	1,472
Age (mean ± sd)	75.1 ± 5.4	72.4 ± 5.7	71.2 ± 7.1	73.9 ± 7.6	75.1 ± 8.0	73.9 ± 7.2
Sex (M/F)	182/159	36/49	147/118	306/189	162/124	833/639

After pre-processing and matching the subjects among the genotyping data, demographic data and imaging data, there are 1,472 participants ($N = 1,472$) in our study, including 341 cognitively normal (CN), 85 with significant memory concern (SMC), 265 with early mild cognitive impairment (EMCI), 495 late MCI (LMCI), and 286 AD subjects. A brief characteristic description of the participants is shown in Table 1.

Structural MRI scans were processed with voxel-based morphometry (VBM) using the Statistical Parametric Mapping (SPM) software tool.[17] All scans were aligned to a T1-weighted template image, segmented into gray matter (GM), white matter (WM) and cerebrospinal fluid (CSF) maps, normalized to the standard Montreal Neurological Institute (MNI) space as 2×2×2 mm³ voxels. The GM maps were extracted and smoothed with an 8mm FWHM kernel, and analyzed in this study. A total of 185,405 non-background voxels, covering cortical, sub-cortical, and cerebellar regions and measuring GM density, were studied in this work as voxel-level imaging traits. Based on the AAL atlas,[18] 116 ROI-level traits were also obtained by averaging all the voxel-level measures within each ROI.

For the genotyping data, we performed quality control (QC) using the following criteria: genotyping call rate > 95%, minor allele frequency > 5%, and Hardy-Weinberg Equilibrium > 1e-6. After the QC, rs429358 (APOE) SNP is added to the genotyping data. We extracted 54 AD related SNPs, which were reported in the main text of at least one of the three landmark AD genetics studies.[19–21] 54 AD non-related SNPs were also extracted serving for the comparison purpose. For the AD non-related SNPs, we first downloaded the AD related SNP list from DisGeNet (`www.disgenet.org`)[22] which includes 1,843 SNPs. Our 54 AD non-related SNPs are randomly selected from our genotyping data so that none of those belongs to the above 54 selected AD related SNPs and the 1,843 DisGeNet AD SNPs.

4. Experimental Design

Our overall experimental pipeline is presented in Figure 1. The pipeline is designed to compare two strategies to identify imaging genetic associations via ROI-based regional morphometricity estimation for each of 54 AD related SNPs and 54 non-AD related SNPs. As mentioned earlier, the first strategy constructs the ASM using a univariate average measure for the ROI, and the second strategy constructs the ASM using all the multivariate voxel measures within the ROI. We expect that the second strategy provides improved detection power.

Starting from the 3D voxel-based morphometric measurements, we first remove the background voxels (defined by voxels without any signal across all the subjects), and then vecterize
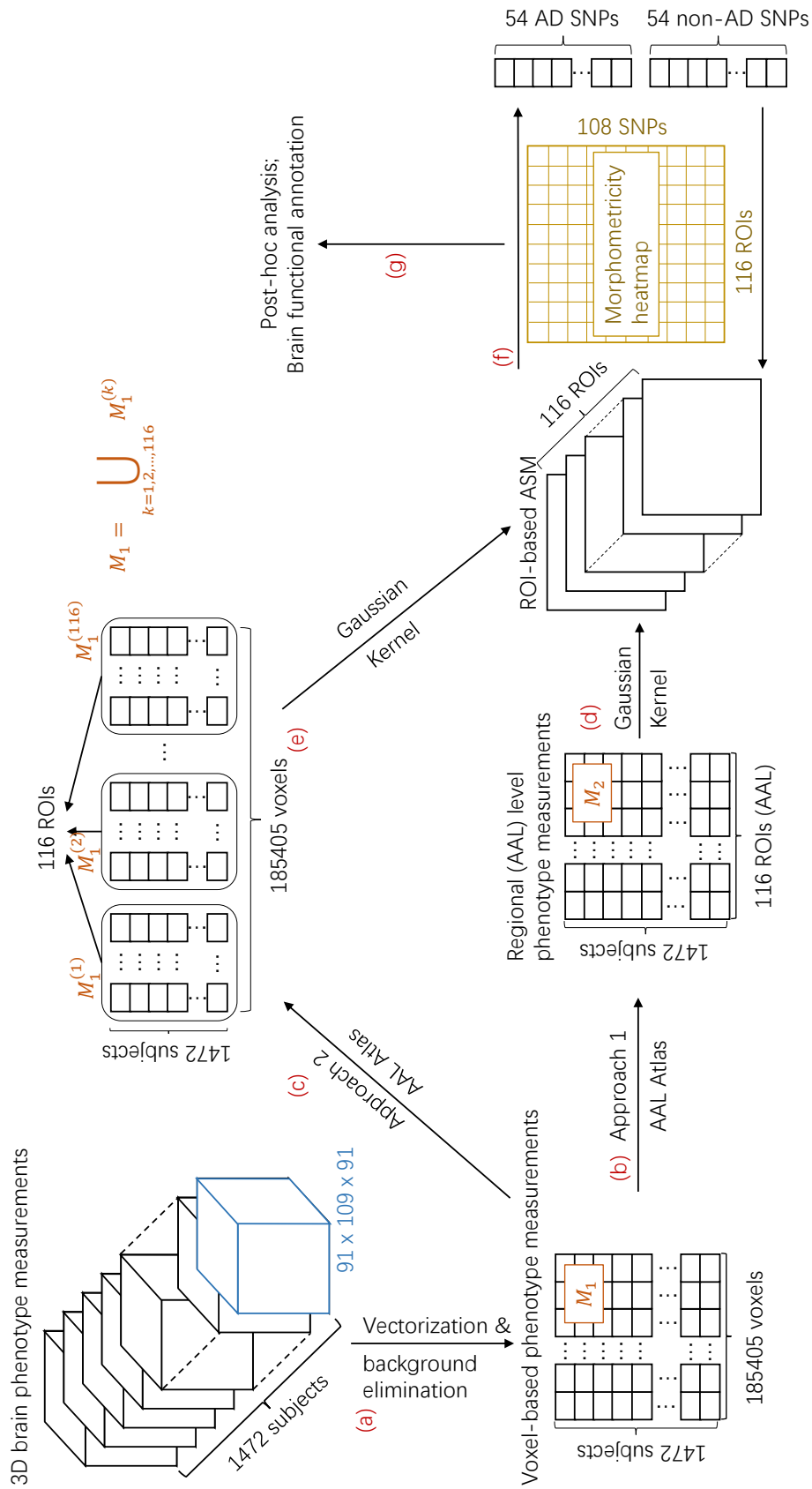
Fig. 1: **Pipeline for genetic variants prioritization evaluation.**
Note: "# of" represents "the number of".

all the remaining voxels in Step (a). As a result, a subject-by-voxel morphometric data matrix is obtained (M_1 in Figure 1).

In Step (b), we map the voxel-level measurements to ROI-level measurements according to the AAL atlas, where the ROI-level measurements are obtained by averaging the voxel-level VBM measurements across all the voxels within the ROI (M_2 in Figure 1). Next, we calculate the ASM matrices in Step (d) by applying the Gaussian kernel defined in Section 2 to each single ROI measurement vector (i.e., each column in M_2).

Besides the above baseline method (Approach 1), as mentioned earlier, we also propose a more advanced approach (Approach 2) to more accurately capture the subject-subject similarity when calculating the ASM. Specifically, instead of averaging the voxel-level measures within each ROI in Step (b), we group the voxels without averaging in Step (c) and use all the multivariate voxel-level imaging measures within each ROI (i.e., $M_1^{(1)}$, $M_1^{(2)}$, ..., $M_1^{(116)}$ in Figure 1) to calculate the ASM for the ROI in Step (e). Note that the matrix M_1 is equivalent to the concatenation of all the matrices $M_1^{(1)}$, $M_1^{(2)}$, ..., $M_1^{(116)}$; and the kth ROI-level phenotype measurement in M_2 is exactly equal to the mean of all the voxel-level measurements within the kth ROI ($M_1^{(k)}$ in Figure 1).

After that, in Step (f), the regional morphometricity for each of 54 AD SNPs and 54 non-AD SNPs is calculated using the ASMs, and a heatmap showing the regional morphometricity is reported. Finally, in Step (g), we use a Fisher's exact test and brain functional annotation to demonstrate that the second approach for ASM calculation is able to capture more interesting imaging genetics associations than the first approach. Here the goal of the Fisher's exact test on each ROI is to assess whether AD-related SNPs tend to have a higher regional morphometricity on the ROI. The identification of ROIs with such a pattern can help us explore the underlying molecular pathway from SNPs to brain structure, and to AD outcome.

All the analysis is performed using the implementation from the existing study[9] (`people.csail.mit.edu/msabuncu/morphometricity/`) with our modification to add the calculation of p-value using a likelihood ratio test.[9] Our ASMs are computed using the Gaussian kernel.

5. Results and Discussion

Figure 2 and Figure 3 show the SNP morphometricity on each ROI calculated using Approach 1 and Approach 2 respectively. Rows of the heatmap represent the 108 SNPs (54 AD SNPs and 54 non-AD SNPs) by their rs numbers, and columns of the heatmap represent 116 brain ROIs. Our current results indicate that the AD-related SNPs have higher overall regional morphometricity estimates than the SNPs not yet related to AD. This observation suggests that the variances of AD SNPs can be explained more by regional morphometric features than non-AD SNPs, supporting the value of imaging traits as targets in studying AD genetics to study AD genetics.

To better visualize the difference between the estimated morphometricity between non-AD SNPs and AD SNPs, we further pooled the morphometricity for SNPs among 116 ROIs into two big groups according to their relations with AD and plot the histogram and density plot to visualize the distribution of the morphometricity of two groups. The histogram and density plots are shown in Figure 4. Although a large proportion of SNP morphometricity
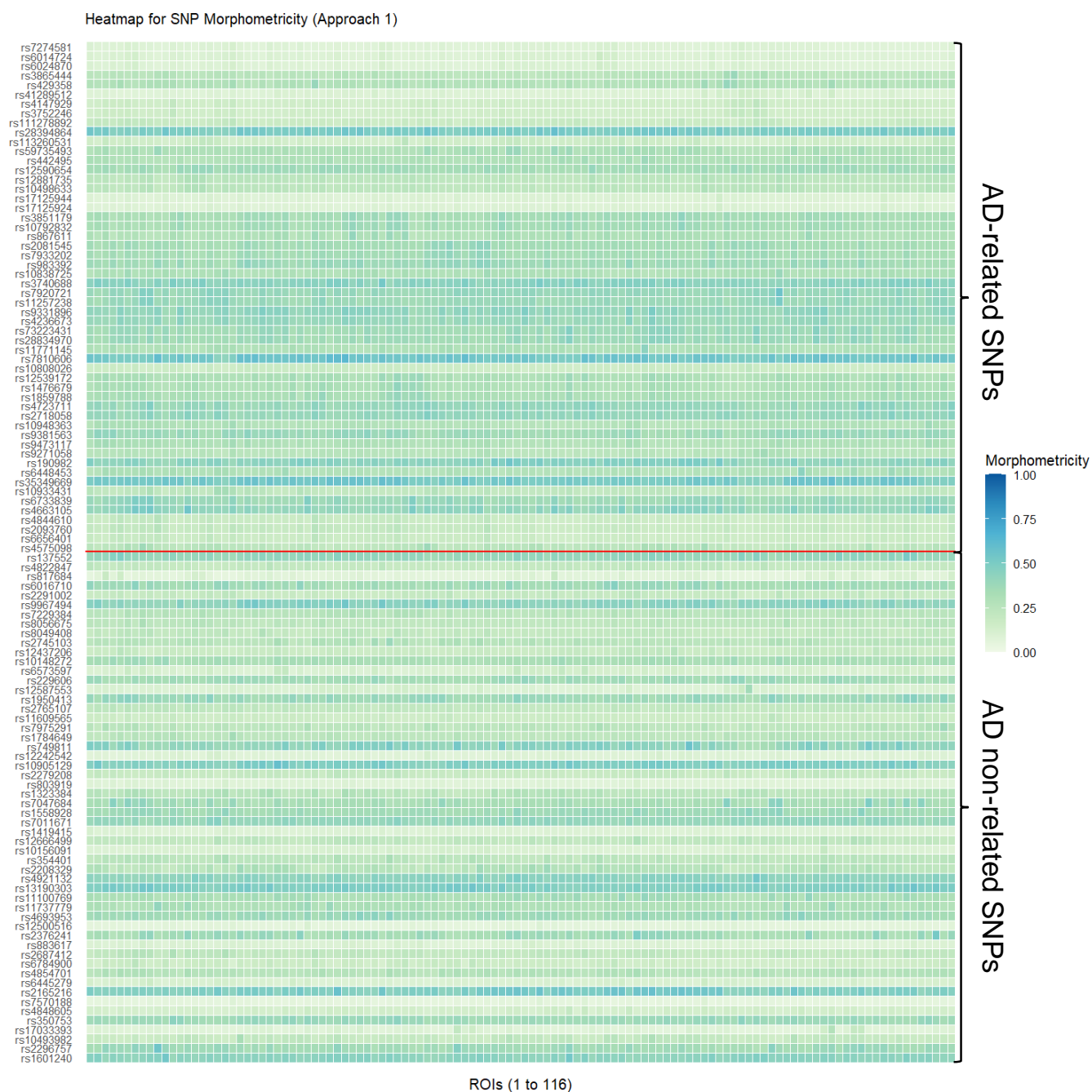
Fig. 2: **Heatmap for SNP morphometricity on each ROI (Approach 1).** This heatmap has dimension 108×116 where each row represents a SNP and each column represents an ROI (ROI 1 at the first column till ROI 116 at the last column). Color represents the estimated morphometricity value for the corresponding SNP and ROI. The red line separates the AD-related SNPs and AD non-related SNPs.

overlaps with each other, the distribution for the AD related SNP group shows an overall higher morphometricity than the non-AD SNP group.
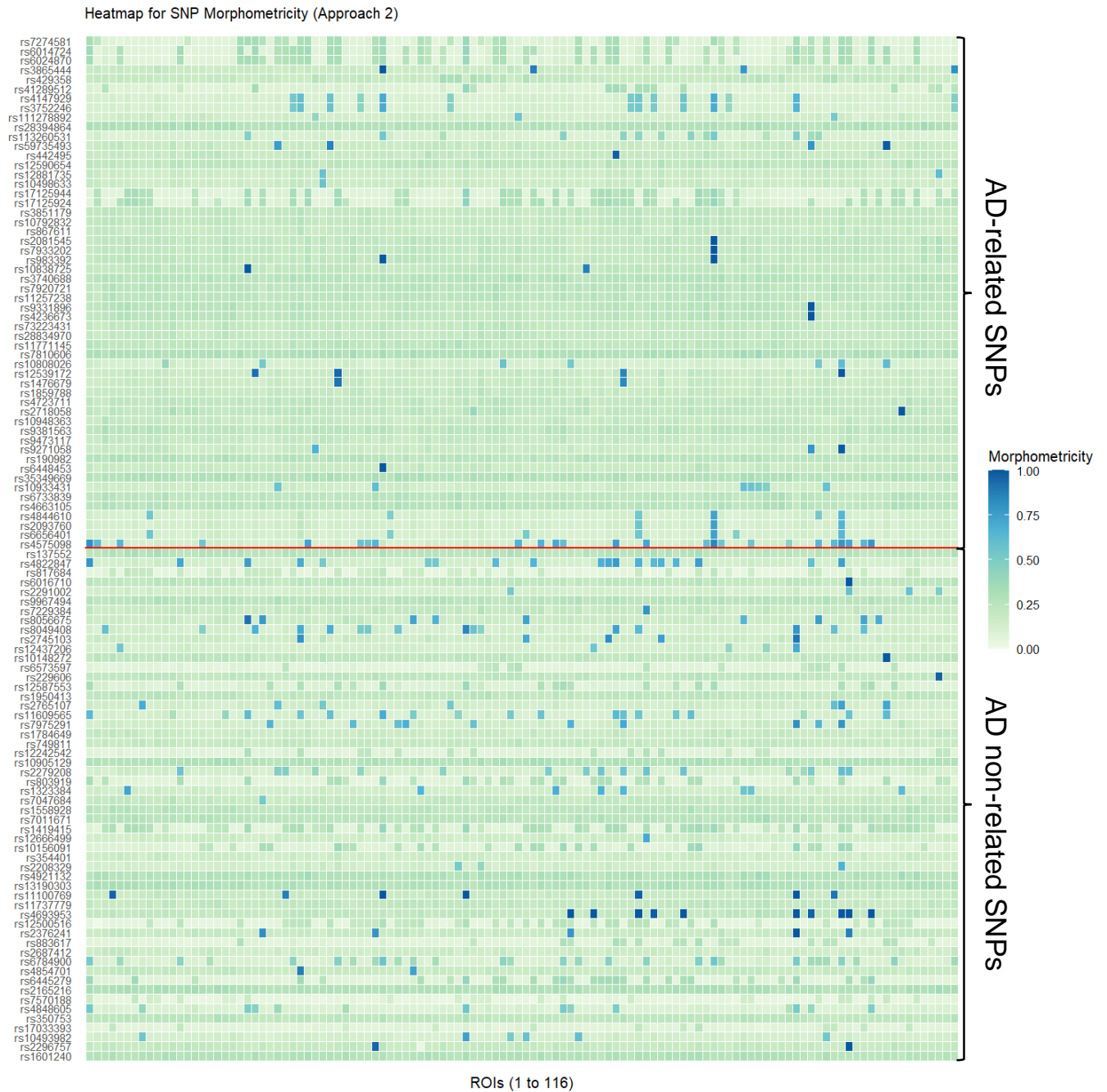
Fig. 3: **Heatmap for SNP morphometricity on each ROI (Approach 2).** This heatmap has dimension 108×116 where each row represents a SNP and each column represents an ROI (ROI 1 at the first column till ROI 116 at the last column). Color represents the estimated morphometricity value for the corresponding SNP and ROI. The red line separates the AD-related SNPs and AD non-related SNPs.

However, a potential issue for Approach 1 is that, compared with the morphometricity distribution for Approach 2 (Figure 4b), the morphometricity distribution for Approach 1

Distribution of Morphometricity (Approach 1)

(a) Distribution of Morphometricity for non-AD SNPs and AD SNPs (Approach 1)
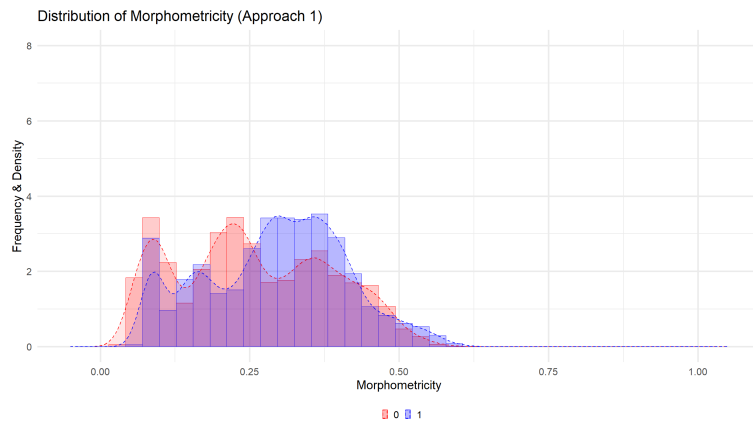
Distribution of Morphometricity (Approach 2)
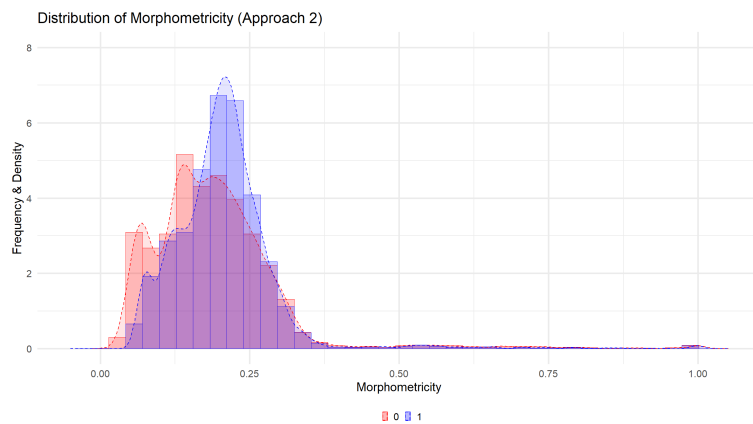
(b) Distribution of Morphometricity for non-AD SNPs and AD SNPs (Approach 2)

Fig. 4: **Comparison of Histogram and Density Plot for non-AD SNPs and AD SNPs Morphometricity.** Figure 4a shows the histogram and density plot for estimated morphometricity using Approach 1; Figure 4b shows the histogram and density plot for estimated morphometricity using Approach 2. Group 0 in each plot denotes the AD non-related SNP group and Group 1 in denotes the AD-related SNP group.

(Figure 4b) overestimates the SNP morphometricity. This can be explained by the restricted maximum likelihood (ReML) algorithm implemented by.[9] In their algorithm, the ASM is required to be non-negative definite and it reconstructes every ASM which is not non-negative definite by eigen-decomposition and changing all the negative eigenvalues to 0. This step will eliminate all the negative relationship between subjects leading to an overall overestimation of morphometricity. In our Approach 1, all the ASMs are calculated from a single univariate ROI measurement vector and all of those matrices are not non-negative definite. Therefore, when calculating the SNP morphometricity for every ROI using Approach 1, all negative relationships between subjects cannot be captured and the SNP morphometricity is overestimated.

To further illustrate the advantages of Approach 2 that it can capture more information with less noise, we performed a post-hoc analysis to test whether a SNP related to AD is associated with the SNP's morphometricity calculated by VBM measurements. In our analysis,
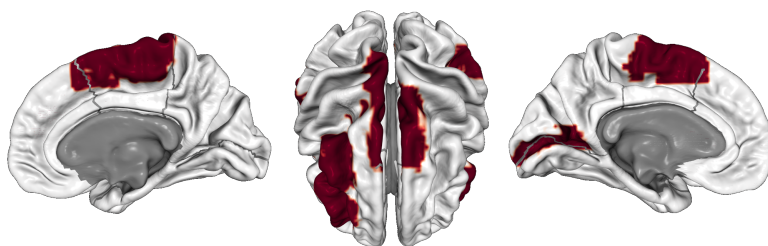
Fig. 5: **Significant ROIs in Approach 2 after the Fisher's exact test.** This brain map highlights the ROIs that are significant (p-value < 0.05) evaluated by the Fisher's exact test. The 11 significant regions are Frontal_Mid_L, Frontal_Inf_Tri_R, Rolandic_Oper_L, Supp_Motor_Area_L, Supp_Motor_Area_R, Calcarine_R, Parietal_Inf_R, SupraMarginal_L, Paracentral_Lobule_L, Cerebellum_Crus2_R, and Cerebellum_9_R.

we first adjusted the p-value for morphometricity estimation using Bonferroni correction. Then for each ROI, we conduct a Fisher's exact test according to the number of AD/non-AD SNPs that have a significant/insignificant morphometricity estimation. Of note, this test is used to examine whether AD SNPs tend to have more significant morphometricity estimation than non-AD SNPs for each ROI. The identified ROIs can be prioritized as valuable imaging traits to study AD genetics. Among all 116 Fisher's exact tests, none of the tests reaches the significance level of 0.05 in Approach 1 whereas 11 (Figure 5) out of the 116 tests in Approach 2 show strong evidence (p-value < 0.05) that the AD/non-AD SNPs and significant/insignificant morphometricity estimation are dependent. This provides us valuable information to guide our search for meaningful AD underlying biological mechanisms (e.g., from SNPs to brain structure and to diagnostic outcome).

We performed brain imaging functional annotation analysis to the 11 significant ROIs using Neurosynth[23] and NeuroVault.[24] Supplementary motor area (SMA), which is a part of primate cerebral cortex, is enriched by the 11 ROIs with voxel-based Pearson correlation 0.217. Evidence has shown that neuromotor function is altered in AD patients during motor behaviors and individuals without dementia exhibit greater activation in SMA.[25] Besides SMA, dorsolateral prefrontal cortex (DPC) is also correlated with our 11 significant ROIs with voxel-based Pearson correlation 0.183. It has been shown that AD patients tend to have impaired extent of DPC plasticity compared to the non-AD individuals where the DPC has a significant impact on the patients' working memory.[26] All these existing AD-related findings support the validity of our proposed prioritization method.

6. Conclusion

In this work, we proposed a novel strategy to identify SNP-ROI associations via regional morphometricity by extending the existing morphometricity work from its original definition at the whole brain level to a more focal level based on a region of interest (ROI). We proposed two approaches to incorporate ROI-level morphometric information. Approach 1 employed only a single average ROI measure, while Approach 2 embraced all the detailed voxel-level measures within the ROI. We performed an empirical study on the structural MRI and genotyping data from the landmark ADNI biobank; and yielded promising results. Our findings

indicated that the AD-related SNPs had higher overall regional morphometricity estimates than the SNPs not yet related to AD. This observation suggests that the variances of AD SNPs can be explained more by regional morphometric features than non-AD SNPs, supporting the value of imaging traits as targets in studying AD genetics. In addition, we identified 11 ROIs, where the AD/non-AD SNPs and significant/insignificant morphometricity estimation of the corresponding SNPs in these ROIs were dependent. Supplementary motor area (SMA) and dorsolateral prefrontal cortex (DPC) were enriched by these ROIs. Our results also demonstrated that the proposed Approach 2 captured the ROI information more accurately than Approach 1, and thus had improved power to detect imaging genetic associations.

Acknowledgements

References

1. A. R. Hariri and D. R. Weinberger, Imaging genomics, *British Medical Bulletin* **65**, 259 (03 2003).
2. R. Bogdan, B. J. Salmeron, C. E. Carey, A. Agrawal, V. D. Calhoun, H. Garavan, A. R. Hariri, A. Heinz, M. N. Hill, A. Holmes, N. H. Kalin and D. Goldman, Imaging genetics and genomics in psychiatry: A critical review of progress and potential, *Biological Psychiatry* **82**, 165 (2017), Alterations in Cortical Development in Autism Spectrum Disorder.
3. L. Shen and P. M. Thompson, Brain imaging genomics: Integrated analysis and machine learning, *Proceedings of the IEEE* **108**, 125 (2020).
4. M. Kim, J. Bao, K. Liu, B. yong Park, H. Park, J. Y. Baik and L. Shen, A structural enriched functional network: An application to predict brain cognitive performance, *Medical Image Analysis* **71**, p. 102026 (2021).
5. L. Du, H. Huang, J. Yan, S. Kim, S. L. Risacher, M. Inlow, J. H. Moore, A. J. Saykin, L. Shen and Alzheimer's Disease Neuroimaging Initiative, Structured sparse canonical correlation analysis for brain imaging genetics: an improved GraphNet method, *Bioinformatics* **32**, 1544 (01 2016).
6. L. Du, K. Liu, X. Yao, S. L. Risacher, J. Han, A. J. Saykin, L. Guo and L. Shen, Detecting genetic associations with brain imaging phenotypes in Alzheimer's disease via a novel structured SCCA approach, *Medical Image Analysis* **61**, p. 101656 (2020).
7. X. Yao, S. Cong, J. Yan, S. L. Risacher, A. J. Saykin, J. H. Moore, L. Shen, UK Brain Expression Consortium and Alzheimer's Disease Neuroimaging Initiative, Regional imaging genetic enrichment analysis, *Bioinformatics* **36**, 2554 (12 2019).
8. P. M. Visscher, W. G. Hill and N. R. Wray, Heritability in the genomics era–concepts and misconceptions, *Nat Rev Genet* **9**, 255 (2008).
9. M. R. Sabuncu, T. Ge, A. J. Holmes, J. W. Smoller, R. L. Buckner, B. Fischl and Alzheimer's Disease Neuroimaging Initiative, Morphometricity as a measure of the neuroanatomical signature of a trait, *Proceedings of the National Academy of Sciences* **113**, E5749 (2016).
10. R. Kong, J. Li, C. Orban, M. R. Sabuncu, H. Liu, A. Schaefer, N. Sun, X.-N. Zuo, A. J. Holmes, S. B. Eickhoff and B. T. T. Yeo, Spatial Topography of Individual-Specific Cortical Networks Predicts Human Cognition, Personality, and Emotion, *Cerebral Cortex* **29**, 2533 (05 2018).

11. J. Seidlitz, F. Váša, M. Shinn *et al.*, Morphometric similarity networks detect microscale cortical organization and predict inter-individual cognitive variation, *Neuron* **97**, 231 (2018).

12. J. Li, R. Kong, R. Liégeois, C. Orban, Y. Tan, N. Sun, A. J. Holmes, M. R. Sabuncu, T. Ge and B. T. Yeo, Global signal regression strengthens association between resting-state functional connectivity and behavior, *NeuroImage* **196**, 126 (2019).

13. J. D. Bijsterbosch, M. W. Woolrich, M. F. Glasser, E. C. Robinson, C. F. Beckmann, D. C. Van Essen, S. J. Harrison and S. M. Smith, The relationship between spatial configuration and functional connectivity of brain regions, *eLife* **7**, p. e32992 (Feb 2018).

14. A. J. Saykin, L. Shen, X. Yao, S. Kim, K. Nho, S. L. Risacher, V. K. Ramanan, T. M. Foroud, K. M. Faber, N. Sarwar, L. M. Munsie, X. Hu, H. D. Soares, S. G. Potkin, P. M. Thompson, J. S. Kauwe, R. Kaddurah-Daouk, R. C. Green, A. W. Toga, M. W. Weiner and Alzheimer's Disease Neuroimaging Initiative, Genetic studies of quantitative MCI and AD phenotypes in ADNI: Progress, opportunities, and plans, *Alzheimers Dement* **11**, 792 (2015).

15. L. Shen, P. M. Thompson, S. G. Potkin, L. Bertram, L. A. Farrer, T. M. Foroud, R. C. Green, X. Hu, M. J. Huentelman, S. Kim, J. S. Kauwe, Q. Li, E. Liu, F. Macciardi, J. H. Moore, L. Munsie, K. Nho, V. K. Ramanan, S. L. Risacher, D. J. Stone, S. Swaminathan, A. W. Toga, M. W. Weiner, A. J. Saykin and Alzheimer's Disease Neuroimaging Initiative, Genetic analysis of quantitative phenotypes in AD and MCI: imaging, cognition and biomarkers, *Brain Imaging Behav* **8**, 183 (2014).

16. M. W. Weiner, D. P. Veitch, P. S. Aisen, L. A. Beckett, N. J. Cairns, R. C. Green, D. Harvey, C. R. Jack, J. C. Morris *et al.*, Recent publications from the Alzheimer's Disease Neuroimaging Initiative: Reviewing progress toward improved AD clinical trials, *Alzheimer's & Dementia* **13**, e1 (2017).

17. J. Ashburner and K. J. Friston, Voxel-based morphometry–the methods, *Neuroimage* **11**, 805 (2000).

18. N. Tzourio-Mazoyer, B. Landeau, D. Papathanassiou, F. Crivello, O. Etard, N. Delcroix, B. Mazoyer and M. Joliot, Automated anatomical labeling of activations in SPM using a macroscopic anatomical parcellation of the MNI MRI single-subject brain, *Neuroimage* **15**, 273 (2002).

19. J.-C. Lambert *et al.*, Meta-analysis of 74,046 individuals identifies 11 new susceptibility loci for Alzheimer's disease, *Nature Genetics* **45**, 1 (10 2013).

20. B. Kunkle, B. Grenier-Boley *et al.*, Genetic meta-analysis of diagnosed Alzheimer's disease identifies new risk loci and implicates Aβ, tau, immune and lipid processing, *Nature Genetics* **51**, 414 (03 2019).

21. I. Jansen, J. Savage *et al.*, Genome-wide meta-analysis identifies new loci and functional pathways influencing Alzheimer's disease risk, *Nature Genetics* **51** (03 2019).

22. J. Piñero, J. M. Ramírez-Anguita, J. Saüch-Pitarch, F. Ronzano, E. Centeno, F. Sanz and L. I. Furlong, The DisGeNET knowledge platform for disease genomics: 2019 update, *Nucleic Acids Research* **48**, D845 (11 2019).

23. T. Yarkoni, R. Poldrack, T. Nichols, D. Van Essen and T. Wager, Large-scale automated synthesis of human functional neuroimaging data, *Nature Methods* **8**, 665 (06 2011).

24. K. J. Gorgolewski, G. Varoquaux *et al.*, Neurovault.org: a web-based repository for collecting and sharing unthresholded statistical maps of the human brain, *Frontiers in Neuroinformatics* **9**, p. 8 (2015).

25. E. Vidoni, G. Thomas, R. Honea, N. Loskutova and J. Burns, Evidence of altered corticomotor system connectivity in early-stage Alzheimer's disease, *J Neurol Phys Ther* **36**, p. 1 (2012).

26. S. Kumar, R. Zomorrodi *et al.*, Extent of Dorsolateral Prefrontal Cortex Plasticity and Its Association With Working Memory in Patients With Alzheimer Disease, *JAMA Psychiatry* **74**, 1266 (12 2017).